Technical Report: Input data for GLM simulations of Lake Baratz and Lake Ammersee

S1 Input data for Lake Baratz

S1.1 Observation stations

Meteorological data are taken from several stations in the environment of the lake including an observation station rafting on the lake surface center. Hydrological data (discharge and water temperature) were surveyed at a stream gauge at the Grifone site, where the observation setup was demolished on 31.05.2017. Fig. 3 (main paper) gives an overview of the locations of the stations. The lake station was not in operation from 24.09.2013 to 25.04.2014 (Giadrossich et al., 2015). A detailed description of the source and required processing steps of the respective parameters is given in the section S1.2.

S1.2 Meteorological model input data

S1.2.1 Air temperature

Input data for air temperature are taken from the respective station in the following order:

- Lake station Calculated from Grifone station by linear regression of the lake station ($R^2 = 0.97$, reference period: 25.04.2014 – 31.05.2017, Fig. S1a)
- Calculated from Fertilia station by linear regression of the lake station ($R^2 = 0.99$, reference period: 15.01.2015 – 12.02.2018, Fig. S1b). Values at Fertilia station were available in a precision of 1 degree.
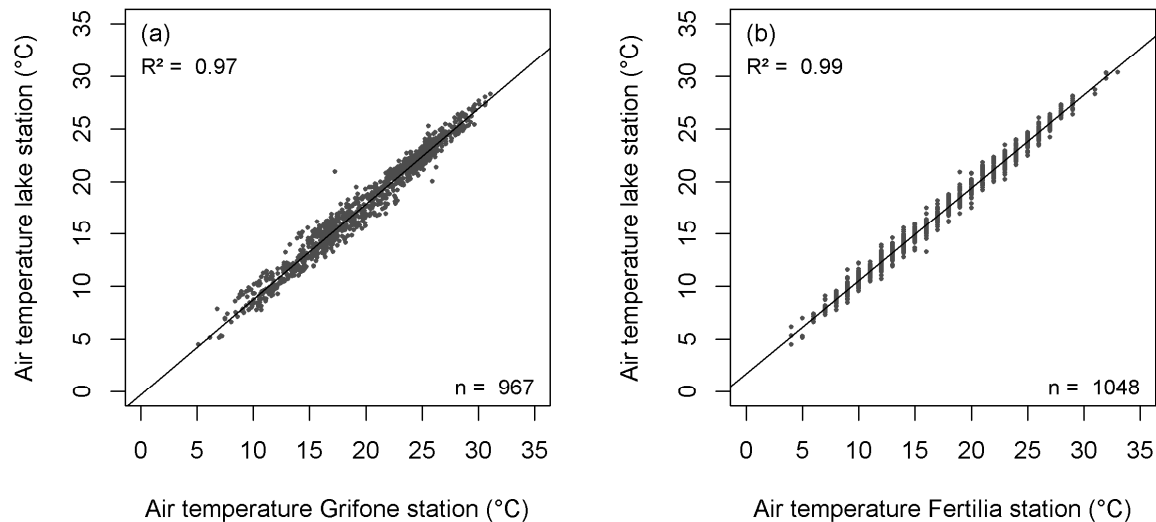

Fig. S1: Linear correlation of air temperature for the lake station and a) Grifone station and b) Fertilia station.

S1.2.2 Wind speed

Wind speed data at the lake station have several observations gaps and the measurements show a significant bias between the periods before and after 21.06.2016 (Fig. S2), when a new sensor was installed after an outage. The bias is detected by comparing to data obtained at Fertilia station. For the period before this date the average wind

speeds measured at the lake station were 1.19 ms^{-1} (average difference) lower than measured at Fertilia station. After the 21.06.2016 the average difference was only 0.08 ms^{-1}. Observations at Grifone station are within the range of the measurements taken at the lake station before 21.06.2016, hence these data were taken as reference for correction.
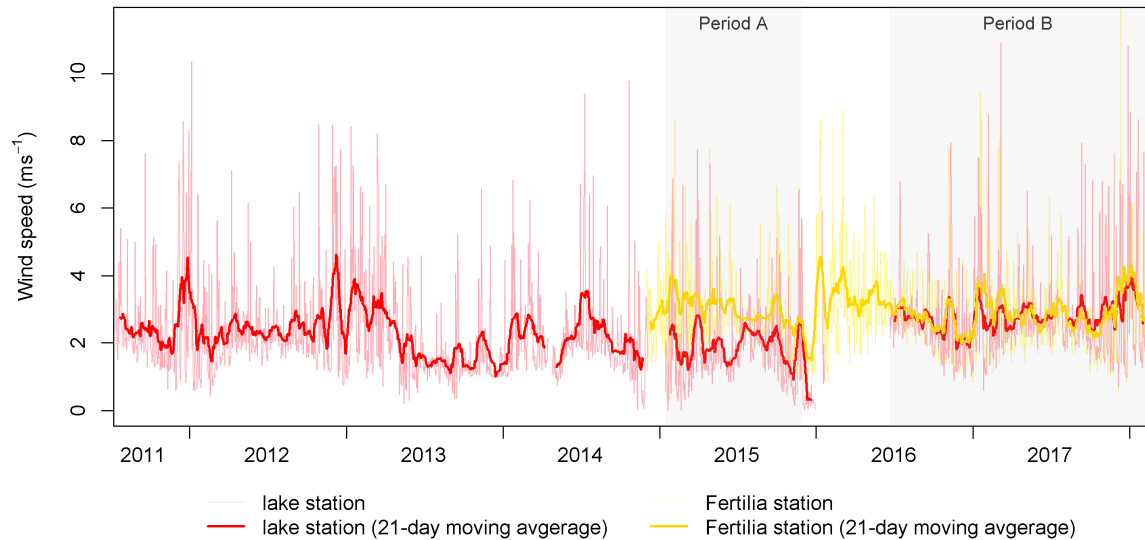
Fig. S2: Time series of daily wind speeds at lake and Fertilia station. Periods A and B are used for mean value comparison (see Table S1)

Table S1: Averages of wind speed at lake and Fertilia station

Period	lake station	Fertilia station
15.01.2015 - 30.12.2015 (period A, Fig. S2)	1.82	3.01
21.06.2016 - 12.02.2018 (period B, Fig. S2)	2.71	2.79

The final time series of wind speed input data (daily values) were prepared first by filling gaps of observations by linear correlation (Table S2), and secondly by adjusting of the values after the 21.06.2016 by multiplying with the factor of 0.67, which is equal to the quotient of the average data for periods before and after at the raft station (see Table S1).

Table S2: Gaps of observations for wind speed at the lake station, station from which data were used, and coefficient of correlation

| Period of data gap	Data source	Reference period	R²	Comment
24.09.2013 – 24.04.2014	Grifone	08.07.2011 – 23.09.2013	0.72	(Giadrossich et al., 2015)
04.12.2014 – 14.01.2015	Fertilia	21.06.2016 – 12.02.2018	0.53	see Fig. S3a
31.05.2015 – 20.06.2016	Fertilia	15.01.2015 – 30.12.2015	0.41	see Fig. S3b
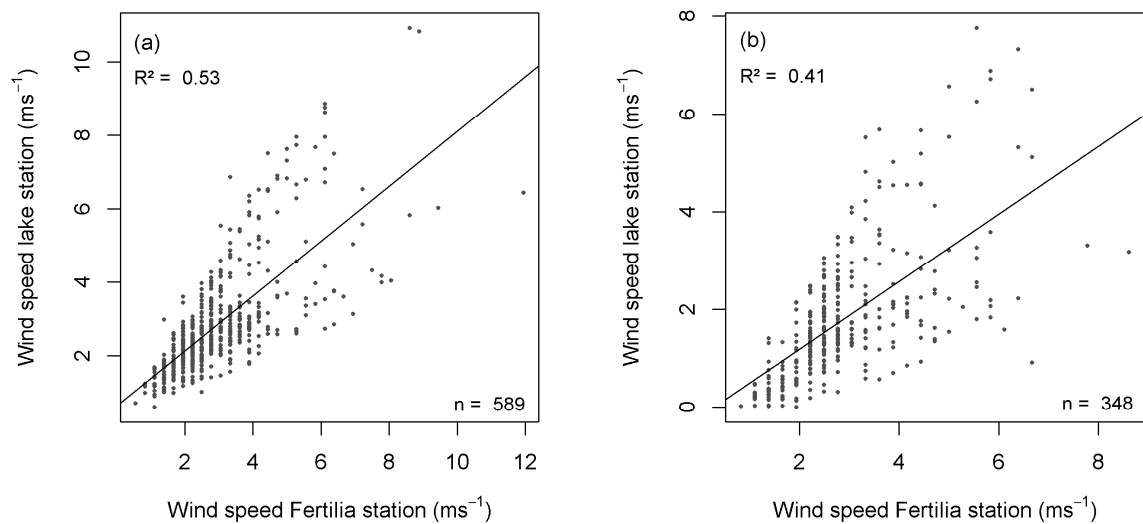
Fig. S3: Linear correlation of wind speed for the lake and Fertilia station, a) period 21.06.2016 to 11.02.2018, b) 15.01.2015 to 30.12.2015

S1.2.3 Relative humidity

Missing data for the lake station were filled by linear correlation. Table S3 gives an overview on the interpolated gaps and the used data source. The maximum observed value for relative humidity at the lake station is 96.89 %. Values computed from the other stations may exceed this value and were then set to be 97.0 %.

Table S3: Gaps of observations for relative humidity at the lake station, station from which data were used, and coefficient of correlation

Period of data gap	Data source	Reference period	R^2	Comment
24.09.2013 – 24.04.2014	Grifone	08.07.2011 – 23.09.2013	0.82	(Giadrossich et al., 2015)
04.12.2014 – 14.01.2015	Grifone	24.04.2014 – 03.12.2014	0.80	see Fig. S4a
21.01.2016 – 22.03.2016	Grifone	08.10.2015 – 23.11.2016	0.74	see Fig. S4b
24.11.2016 – 22.03.2017	Fertilia	24.03.2017 – 20.11.2017	0.89	see Fig. S4c
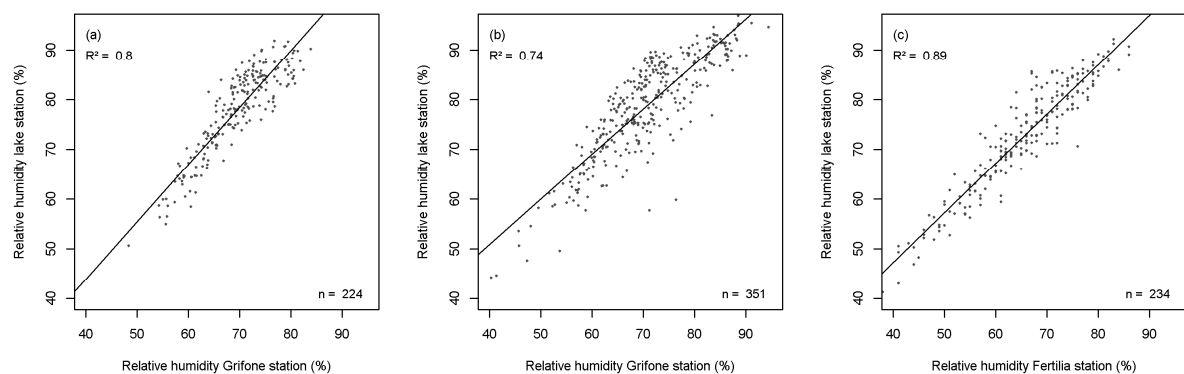
Fig. S4: Linear correlation of relative humidity for the lake station and Grifone station (a) period 24.04.2014 – 03.12.2014 and b) period 08.10.2015 – 23.11.2016) and c) Fertilia station.

S1.2.4 Rainfall

No precipitation data are obtained at the lake station. Measurements exist at Grifone site until 31.05.2017. Table S4 shows the gaps in the rainfall time series at Grifone station and the source for filling.

Table S4: Gaps of observations for rainfall at Grifone and information on filling method

Period of data gap	Number of days	Data source (rainfall data)	Filling method/comment
18.08.2013 – 23.08.2013	6	-	assumed to be 0
14.09.2015 – 07.10.2015	24	-	Estimated from soil moisture data at Grifone station
28.11.2016 – 10.12.2016	13	Olmedo & Capo Caccia	Average of the two stations
15.12.2016 – 20.12.2016	6	Olmedo & Capo Caccia	Average of the two stations
12.01.2017 – 09.03.2017	57	Olmedo & Capo Caccia	Average of the two stations
10.03.2017 – 22.03.2017	13	*Not filled*	
01.06.2017 – 31.08.2017	92	-	Assumed to be 0
01.09.2017 – 12.02.2018	193	Capo Caccia	

The mean annual precipitation at Grifone is about 600 mm (Pirastru and Niedda, 2013) and Sardinia is characterized by a rainy winter season and dry summer months (Niedda et al., 2014; Chessa et al., 1999). Hence, periods in summer with no rainfall observations are assumed to be 0.

S1.2.5 Shortwave and longwave radiation

Radiation measurements representing the net radiation are available at lake station and Grifone station. All data gaps at the lake station are filled by linear correlation from Grifone ($R^2 = 0.93$, Fig. S5). Three short gaps with maximum of eight days are filled by linear interpolation. The required (incoming) shortwave R_{Sin} (Wm^{-2}) and longwave (net) radiation R_{Lnet} (Wm^{-2}) are calculated from the net radiation values using the energy balance:

$$R_n = (1 - \alpha) * R_{sin} + R_{Lnet} \tag{1}$$

where R_n is the net radiation (Wm^{-2}), α is the albedo of the water surface (assumed to be 0.2, Hipsey et al., 2014). Net longwave is described as (Hipsey et al., 2017):

$$R_{Lnet} = R_{Lin} - R_{Lout} \tag{2}$$

where R_{Lout} (Wm^{-2}) is the outgoing longwave radiation and R_{Lin} (Wm^{-2}) is the incoming radiation. Based on the Stefan-Boltzmann law the incoming and outgoing longwave can be calculated from the emissivity and temperature of water and air, respectively (An et al., 2017):

$$R_{Lout} = \varepsilon_w * \sigma * (T_s + 273.1)^4 \tag{3}$$

$$R_{Lin} = \varepsilon_a * \sigma * (T_a + 273.1)^4 \tag{4}$$

where ε_w the emissivity of the water surface, assumed to be 0.985 (Hipsey et al., 2017), ε_a is the air emissivity, σ is the Stefan-Boltzman constant, T_S is the surface water temperature (°C), and T_a is the air temperature (°C). For T_s measurements from the lake surface can be used. For days with no observations T_s is calculated from T_a by polynomial regression ($R^2 = 0.88$, Fig. S6):

$$y = -6.154 * 10^{-7} * x^6 + 7.048 * 10^{-5} * x^5 - 3.139 * 10^{-3} * x^4 + 6.572 * 10^{-2} * x^3 - 0.620 \tag{5}$$
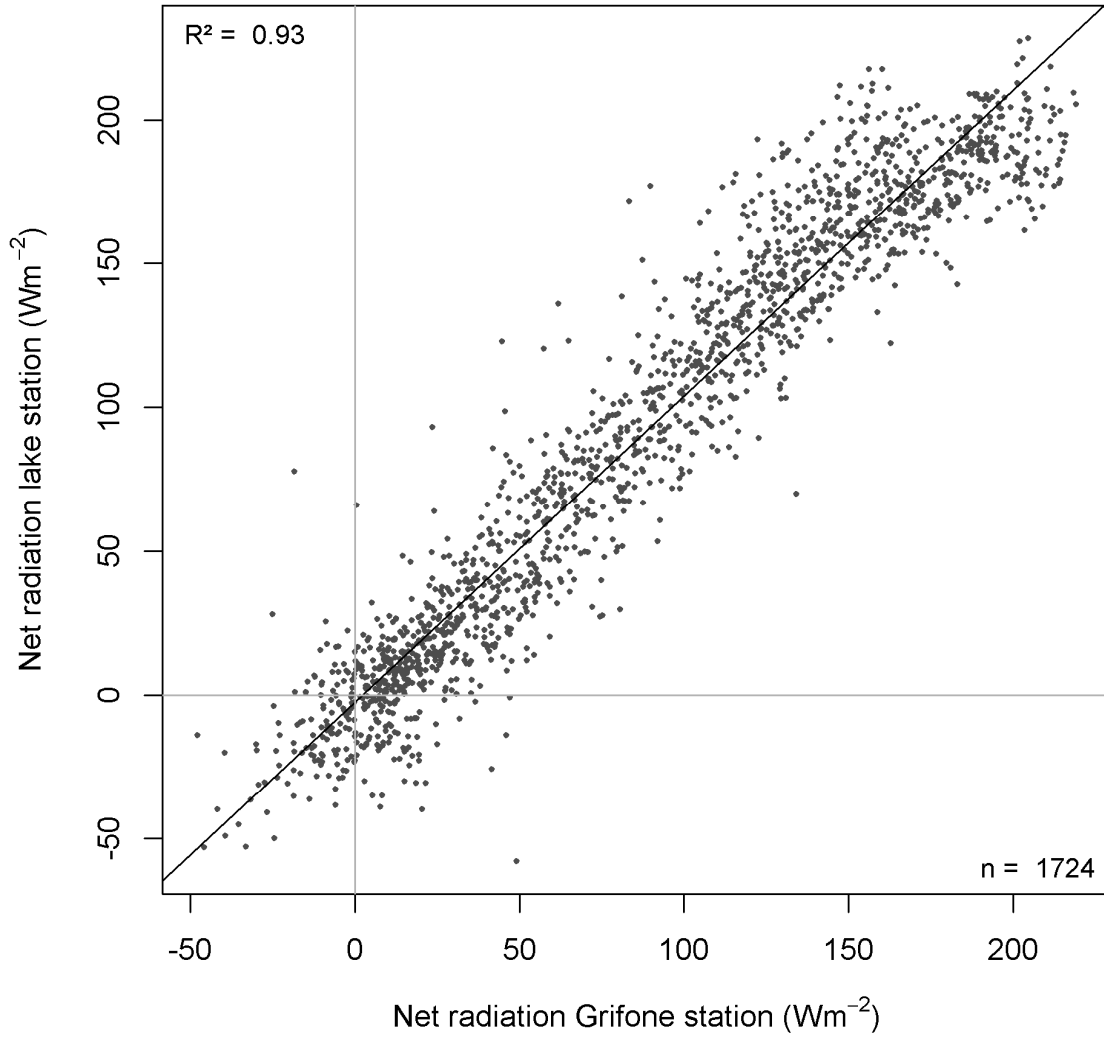$$* x^2 + 2.923 * x + 3.536$$

Air emissivity is calculated using the expression proposed by An et al., (2017, adopted from Idso, 1981):

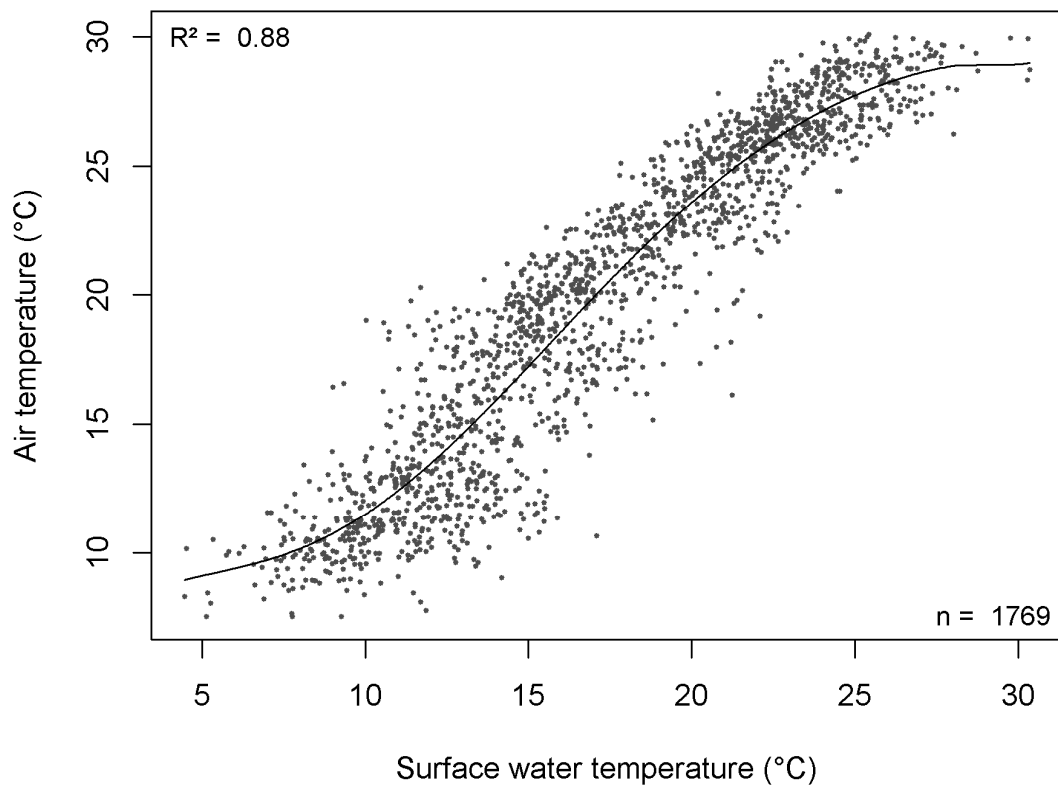$$\varepsilon_a = 0.7 + 5.95 * 10^{-4} * e_a * e^{(1500*(T_a-273.1)^{-1})} \tag{6}$$

$$e_a = \frac{RH}{100} * e_s \tag{7}$$

$$e_s = 0.6107 * e^{17.269*T_a*(T_a+273.1)^{-1}} \tag{8}$$

where e_a is the vapor pressure (kPa), RH is the relative humidity (%) of air, and e_s is the saturated vapor pressure (kPa) at T_a.

Fig. S5: Linear correlation of net radiation for the lake station and Grifone station (period: 13.07.2011 – 30.05.2017).

Fig. S6: Polynomial correlation for the surface water and air temperature at the lake station (period: 13.07.2011 – 12.08.2018)

The monthly means of the calculated shortwave radiation exhibit only slight deviations to the values presented by Lavangini et al. (1990, Table S5).

Table S5: Monthly mean of shortwave radiation

month	Shortwave radiation (Wm^{-2})	
	Lavagnini et al. (1990)	calculated
Jan	78.1	91.4
Feb	110.0	120.0
Mar	167.8	181.3
Apr	225.7	242.5
May	289.4	293.4
Jun	312.5	318.9
Jul	312.5	309.2
Aug	277.8	280.4
Sep	223.4	211.3
Oct	148.1	148.3
Nov	81.0	95.3
Dec	67.1	83.0

S1.3 Hydrological model input data

S1.3.1 Inflow discharge

Observed discharge data are available for Grifone site. At the cross-section the sub-catchment area of this gauge is 7.4 km², which represents approximately 62 % of the lake watershed. The inflow to the lake is simulated applying the hydrological model developed by Niedda et al. (2014) representing the entire lake catchment. The daily values of the inflow discharge for the GLM simulation are composed of the observed discharge value of Grifone gauge and 38 % of the simulated discharge representing that percentage of the catchment. Periods without observation data are either set to 0 m³s^{-1} during dry seasons or filled based on expert knowledge considering rainfall data (24.01.2014 – 12.02.2014).

S1.3.2 Inflow water temperature

Observations of inflow water temperature exist only at Grifone gauge (see Fig. 3, main paper) for the periods 01.10.2015 – 13.05.2017 and 01.01.2017 – 06.07.2017. Values for periods with no observation data are calculated from the air temperature by subtracting 1.0 °C from the daily mean value of air temperature. The computation by linear correlation was discarded, because the time series of water and air temperature show distinctive different relationships for the two applicable periods (with constant stream runoff, Table S6).

Table S6: Coefficient of correlation and linear relationship for water and air temperature for periods with constant runoff

Period	R²	Linear relationship
27.02.2016 – 13.05.2016	0.29	y = 0.535x + 7.691
17.02.2017 – 11.05.2017	0.84	y = 1.165x - 1.021

S1.3.2 Outflow discharge

The lake has no surface outflow, but an exfiltration to groundwater can be assumed. Niedda et al. (2014) estimate a seepage value of 1.5 mm per day, which is represented by a constant outflow time series in the input data. The average lake surface area of 0.38 km² for the period of July 2011 to August 2017 is applied to calculate the outflow discharge value of 0.0066 ms^{-1}.

S1.4 Lake field data

S1.4.1 Lake level

Lake level data surveyed by means of a diver sensor placed on the lake bottom (further details on the instrument setup see Giadrossich et al. (2015)) with an hourly resolution starting from 18.11.2011. Prior to this date manually measurements are available in a weekly to biweekly resolution. Data from the diver are outputted as height (m) over the lake bottom. The position of the data logger at the lake bottom and thereby its elevation above sea level slightly changes with each re-installation after a data export on the surface. Hence, the data are corrected to refer all heights to the same elevation of 18.85 m a.s.l.. The data taken from the surface are also set to this reference elevation.

S1.4.2 Lake water temperature

Water temperature data were observed automatically by the lake station and are available from 26.08.2012 measuring in the depths of 1, 2, 4, and 6 m in hourly resolution. The surface and bottom water temperature were measured by a diver with an observation start on 26.07.2012 and 23.08.2012, respectively (for further details on the instrument setup see Giadrossich et al. (2015)). From 27.11.2015 also the depths of 3 and 5 m were studied. Prior to the automatically observations temperature profiles were collected manually every 2 to 5 weeks. Fig. S7 visualizes the available filed data of lake water temperature. For the period of 24.09.2013 – 04.03.2014, when the lake station was not in operation (including the diver at the surface), the surface temperature is derived from the bottom temperature based on the assumption of isothermal conditions in the vertical lake profile. Homothermy is common for the site in this season of the year and the vertical temperature gradient of 0.91 °C on 24.09.2014 was already low indicating no stable thermal stratification.
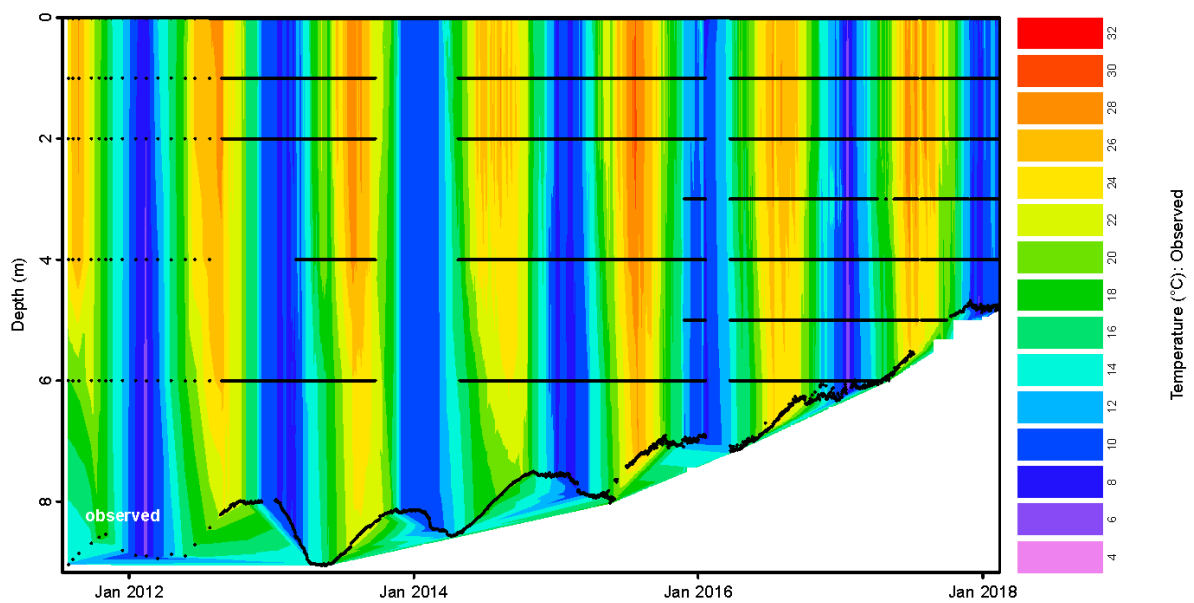

Fig. S7: Visualization of available field data of water temperature (black dots) and interpolated temperatures in the vertical profile (glmGUI).

S2 Input data for Lake Ammersee

S2.1 Observation stations

The locations of hydrological gauging stations (discharge and groundwater) are displayed in Fig. 7 in the main text. Meteorological observation stations are shown in (Fig. S8). Lake field data are surveyed at the Lake station, where also meteorological observations are taken. All data except for cloud cover data (see chapter S2.2) are freely available at https://www.gkd.bayern.de/ provided by the Bavarian Environment Agency (Bay. LfU, 2018).
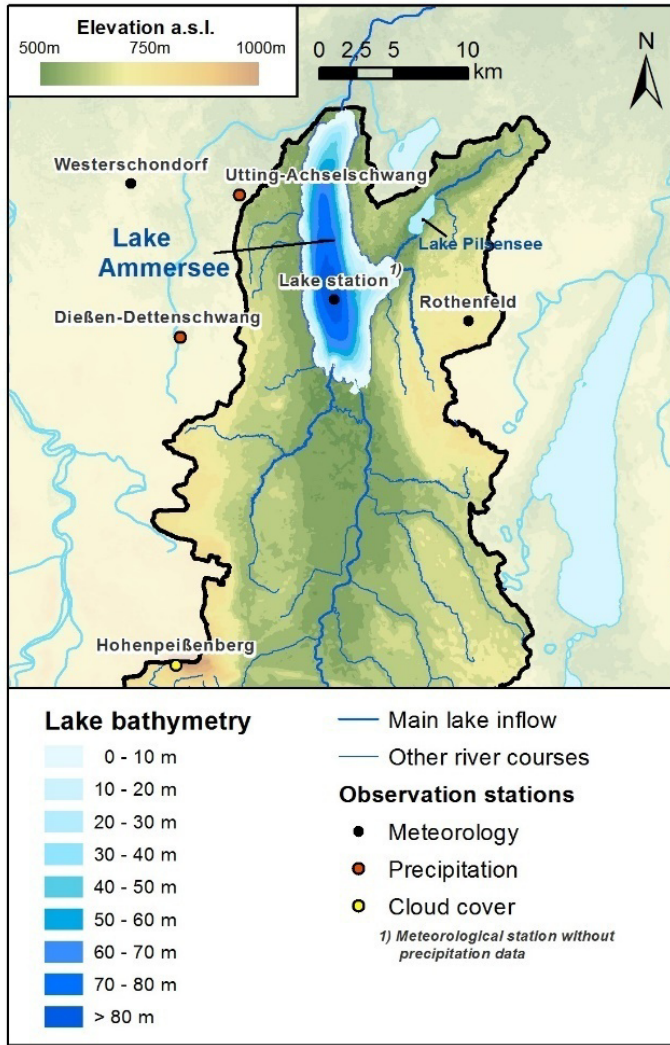
Fig. S8: Bathymetry of Lake Ammersee and meteorological observation stations (Source DEM: Elevation data from ASTER GDEM, a product of METI and NASA, Source geo-data: Geobasisdaten © Bayerische Vermessungsverwaltung, www.geodaten.bayern.de).
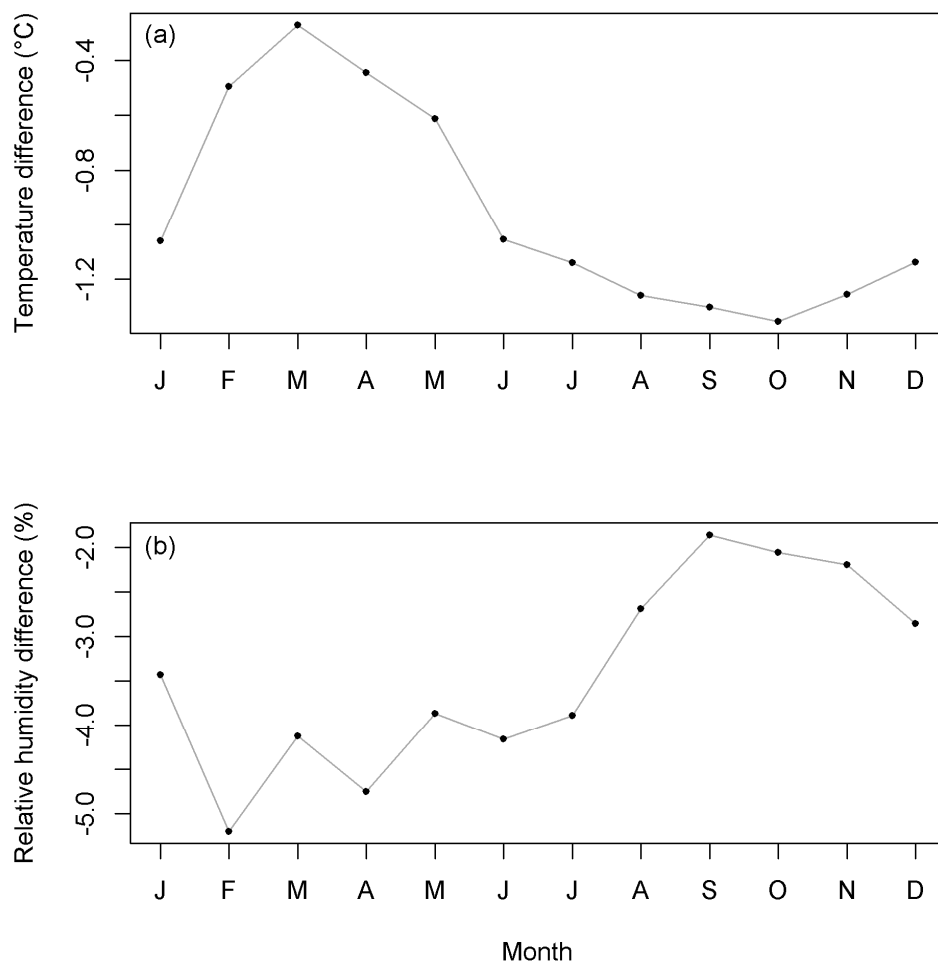
S2.2 Meteorological model input data

Observations of air temperature, wind speed, relative humidity, and shortwave radiation are gathered at the lake station as meteorological input data for the simulation. The parameters are measured in a temporal resolution of 15 minutes. Shortwave radiation data are added to daily sums. For the other three parameters daily averages are calculated.

Missing values for wind speed, air temperature and relative humidity are calculated from observations (hourly values) of Rothenfeld station (Fig. S8). The latter two are subject to considerable seasonal variations in the difference of the measurements between the lake and Rothenfeld station (Fig. S9). Hence, missing values are computed by adding the average deviation for the simulation period of the respective month. The monthly mean values are computed based on a 19-day moving average. Missing data for wind speed are calculated from Rothefeld station observations by adding the mean offest value of the simulation period of -1.3 ms^{-1}. Missing values of shortwave radiation data at the lake station are computed from the average of Rothefeld and Westerschondorf measurements (at both stations hourly observations) and no further error correction is required. Precipitation is inputted to the model as averaged values from observations of the stations Rothefeld, Utting-

Achselschwang, and Dießen-Dettenschwang. According to Springer et al. (2015), the data are recognized as snow as soon as temperatures are below 1.0 °C.

For Lake Ammersee the GLM option of using cloud cover instead of longwave radiation data is selected. The closest location for cloud cover data is Hohenpeißenberg station (Fig. S8, operator: German Weather Service, free available at http://www.dwd.de/cdc, hourly observations) and daily averages are used without correction.

Fig. S9: Average difference (monthly mean of a 19-day moving average) between Rothenfeld and lake station of a) air temperature and b) relative humidity.

S2.3 Hydrological model input data

S2.3.1 Inflow and outflow discharge

Stream discharge is observed only for the two major inflows River Ammer and River Rott plus the River Kienbach (Table S7). The hydrological contribution, concerning quantity and temporal distribution, of River Fischbach, of the other inflows (all other smaller creeks summarized, see Fig. 7 in the main text), and of the groundwater is unknown. To be able to reproduce the lake level applying GLM, four different inflows are defined. The time series represent the discharge data from 1. River Ammer, 2. River Fischbach, 3. groundwater inflow, and 4. the sum of River Rott, River Kienbach, and all other unknown inflows. Hereby, the real contribution of the respective inflow is approached by adjusting the inflow factors during the lake level calibration process.

Values of River Ammer time series are observed at Weilheim station (Fig. 7, main paper). The temporal pattern of Fischbach discharge is highly controlled by the outflow of Lake Pilsensee (Büche, 2018). The discharge of Fischbach is estimated by a simple rainfall-runoff relationship. The hydrograph (Fig. S10) is designed considering the retention of the lake showing a slow reaction of lake outflows on rainfall events (long smoothed decline of discharge) and the subsequent inflow to the water body (indicated by the quick rise of the hydrograph in the first days after the rainfall). With a runoff coefficient of 0.4 the estimated discharge for the simulation period averages to 0.67 m^3s^{-1}. This mean value corresponds to the only hydrological value for Lake Pilsensee existing in the literature of 0.4 m^3s^{-1} for the annual mean of the main inflow (Grimminger, 1982).

Subsurface inflow to Lake Ammersee is estimated from groundwater level observation at Wielenbach (Fig. 7, main paper) calculated by a stage-discharge relation (Fig. S11). The inflow is set to insert the lake at a depth of 79.15 m above the lake bottom, which is about 4 m below the surface (Bueche and Vetter, 2014) dependent on the lake level.

The outflow of Lake Ammersee is observed at gauge station Stegen (Fig. 7, main paper) in a temporal resolution of 15 min. The discharge data are averaged and taken as outflow time series input data. After Kleinmann (1995) no subsurface outflows exist.

Table S7: Characteristics of sub-catchments of Lake Ammersee. The data are representative for the stream inlet to the lake

(Sub)-Catchment	Gauge station	Catchment size (km²)	Percentage of total area (%)
Ammersee	Stegen	994.6	100.0
Other inflows	-	122.0	12.3
Fischbach	-	56.2	5.6
Kienbach	Herrsching	12.4	1.2
Rott	Raisting	82.5	8.3
Ammer	Weilheim	721.5	72.5
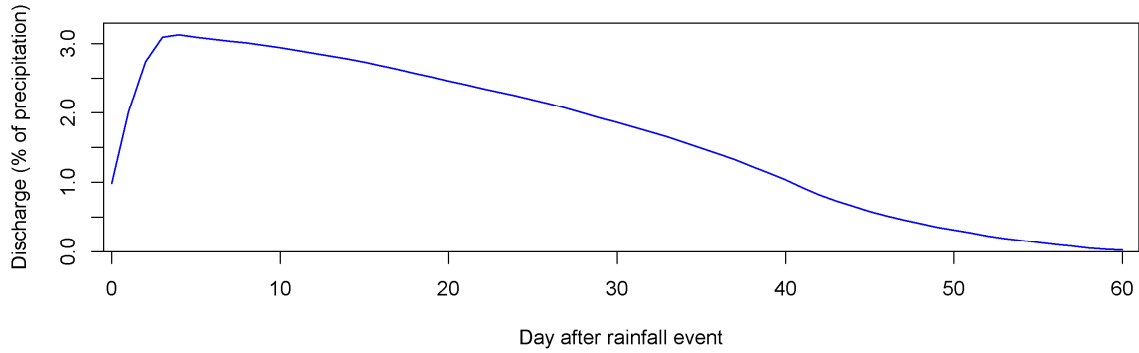
Fig. S10: Hydrograph of River Fischbach for a rainfall event.
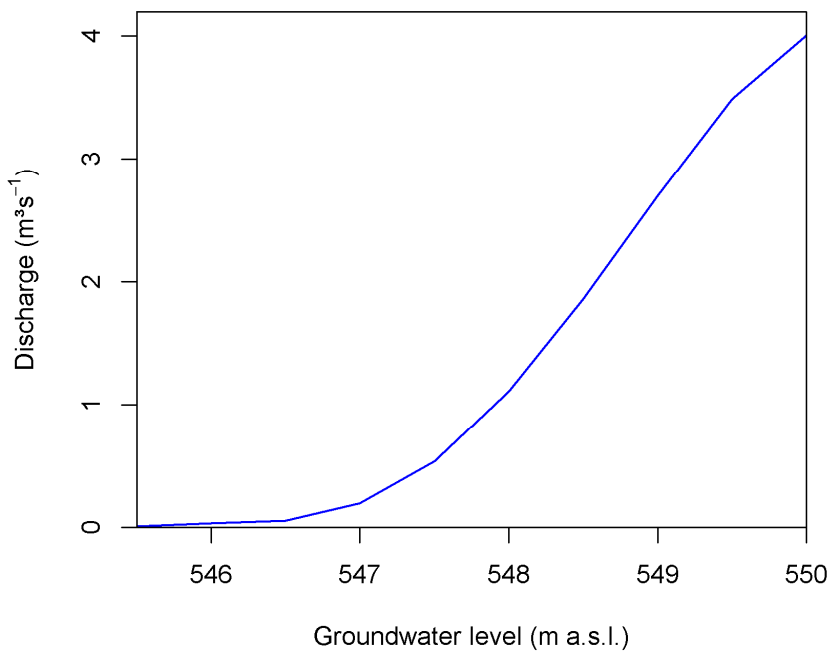
Fig. S11: Stage-discharge relation for groundwater inflow to Lake Ammersee.

The discharge of Rott, Kienbach and all other unknown smaller creeks are defined as one discharge time series to the simulation. Missing values for Rott and Kienbach (maximum gap length = 9 days) are estimated by expert knowledge taking rainfall events into account. The discharge of the smaller inflows is calculated from Kienbach gauge data multiplying the values by the factor of 8.28 representing the relationship of the sub-catchment area sizes. This is feasible as Kienbach and the smaller inflows have similar characteristics in relief and runoff generation.

S2.3.2 Inflow water temperature

Observations for inflow water temperatures are only available for River Ammer surveyed in hourly resolution (Gauge station Weilheim, Fig. 7, main paper) and values for water temperature are only specified for this surface inflow. However, these data can be seen as representative for the sum of all surface inflows. Water temperatures of groundwater can be estimated to be roughly equivalent to the annual air temperature (Boehrer and Schultze,

12

2008) and a constant value of 8.65 °C derived from long-term average air temperature (Bueche and Vetter, 2014) is applied for the subsurface inflow input data.

S2.4 Lake filed data

The water temperatures of the lake are observed automatically by a lake buoy operated by the Bavarian Environment Agency. Data are surveyed in the depths (all in given in m) 0.5 (representing the surface), 1.0, 2.0, 4.0, 6.0, 8.0, 10.0, 12.0, 14.0, 16.0, 18.0, 20.0, 25.0, 40.0, 60.0, and 78.0 in a temporal resolution of 15 min, but already provided by the operator as daily averages. The available data is displayed in Fig. 2 (main paper, black dots) and these values are used as field data. Existing temperature values in May 2016 are evaluated as unrealistic high and excluded from the data set. Lake level data are observed at Stegen gauge station (Fig. 7, main paper) in a temporal resolution of 15 min, but also as daily means are provided. The data unit is elevation a.s.l.. To obtain lake level heights the values are subtracted by the elevation of the lake bottom (449.78 m a.s.l.).

References

An, N., Hemmati, S., and Cui, Y.-J.: Assessment of the methods for determining net radiation at different time-scales of meteorological variables, Journal of Rock Mechanics and Geotechnical Engineering, 9, 239-246, https://doi.org/10.1016/j.jrmge.2016.10.004, 2017.

Bay. LfU, Bayerisches Landesamt für Umwelt: Gewässerkundlicher Dienst Bayern, https://www.gkd.bayern.de/, 2018

Boehrer, B., and Schultze, M.: Stratification of lakes, Reviews of Geophysics, 46, RG2005, 10.1029/2006rg000210, 2008.

Büche, T.: Ableitung des Wasserhaushaltes des Pilsensees aus Niederschlagsdaten - Erste Abschätzungen zum Ausflussgang des Pilsensees., Beiträge zum 49. Jahrestreffen des Arbeitskreises Hydrologie vom 23.-25. November 2017 in Göttingen, *GEOGRAPHICA AUGUSTANA*2018

Bueche, T., and Vetter, M.: Influence of groundwater inflow on water temperature simulations of Lake Ammersee using a one-dimensional hydrodynamic lake model, Erdkunde, 68, 19-31, 10.3112/erdkunde.2014.01.03 2014.

Chessa, P., Cesari, D., and Delitala, A.: Mesoscale precipitation and temperature regimes in Sardinia (Italy) and their related synoptic circulation, Theoretical and applied climatology, 63, 195-221, 1999.

Giadrossich, F., Niedda, M., Cohen, D., and Pirastru, M.: Evaporation in a Mediterranean environment by energy budget and Penman methods, Lake Baratz, Sardinia, Italy, Hydrology and Earth System Sciences, 19, 2451-2468, 10.5194/hess-19-2451-2015, 2015.

Grimminger, H.: Verzeichnis der Seen in Bayern, edited by: Wasserwirtschaft, B. L. f., München, 1982.

Hipsey, M. R., Bruce, L. C., and Hamilton, D. P.: GLM - General Lake Model: Model overview and user information. AED Report #26, The University of Western Australia Technical Manual, 22, 2014.

Hipsey, M. R., Bruce, L. C., Boon, C., Busch, B., Carey, C. C., Hamilton, D. P., Hanson, P. C., Read, J. S., de Sousa, E., Weber, M., and Winslow, L. A.: A General Lake Model (GLM 2.4) for linking with high-frequency sensor data from the Global Lake Ecological Observatory Network (GLEON), Geoscientific Model Development Discussions, 1-60, 10.5194/gmd-2017-257, 2017.

Idso, S. B.: A set of equations for full spectrum and 8- to 14-μm and 10.5- to 12.5-μm thermal radiation from cloudless skies, Water Resources Research, 17, 295-304, doi:10.1029/WR017i002p00295, 1981.

Kleinmann, A.: Seespiegelschwankungen am Ammersee. Ein Beitrag zur spät-und postglazialen Klimageschichte Bayerns, Geologica Bavarica, 99, 253-367, 1995.

Lavagnini, A., Martorelli, S., and Coretti, C.: Monthly maps of daily global incident solar radiation in Italy, Il Nuovo Cimento C, 13, 769-782, 10.1007/bf02507969, 1990.

Niedda, M., Pirastru, M., Castellini, M., and Giadrossich, F.: Simulating the hydrological response of a closed catchment-lake system to recent climate and land-use changes in semi-arid Mediterranean environment, Journal of Hydrology, 517, 732-745, http://dx.doi.org/10.1016/j.jhydrol.2014.06.008, 2014.

Pirastru, M., and Niedda, M.: Evaluation of the soil water balance in an alluvial flood plain with a shallow groundwater table, Hydrological Sciences Journal, 58, 898-911, 10.1080/02626667.2013.783216, 2013.

Springer, J., Ludwig, R., and Kienzle, S. W.: Impacts of Forest Fires and Climate Variability on the Hydrology of an Alpine Medium Sized Catchment in the Canadian Rocky Mountains, Hydrology, 2, 23-47, 10.3390/hydrology2010023, 2015.